Original Article

DOI: 10.5582/bst.2023.01022

Interaction with ERp57 is required for progranulin protection against Type 2 Gaucher disease

Yuzhao Liu[1,2,§], Xiangli Zhao[1,§], Jinlong Jian[1], Sadaf Hasan[1], Chuanju Liu[1,3,*]

[1] Department of Orthopaedic Surgery, New York University Grossman School of Medicine, New York, New York, USA;
[2] Department of Endocrinology, the Affiliated Hospital of Qingdao University, Qingdao, China;
[3] Department of Cell Biology, New York University Grossman School of Medicine, New York, New York, USA.

SUMMARY Gaucher disease (GD), one of the most common lysosomal storage diseases, is caused by *GBA1* mutations resulting in defective glucocerebrosidase (GCase) and consequent accumulation of its substrates β-glucosylceramide (β-GlcCer). We reported progranulin (PGRN), a secretary growth factor-like molecule and an intracellular lysosomal protein was a crucial co-factor of GCase. PGRN binds to GCase and recruits Heat Shock Protein 70 (Hsp70) to GCase through its C-terminal Granulin (*Grn*) E domain, termed as ND7. In addition, both PGRN and ND7 are therapeutic against GD. Herein we found that both PGRN and its derived ND7 still displayed significant protective effects against GD in Hsp70 deficient cells. To delineate the molecular mechanisms underlying PGRN's Hsp70-independent regulation of GD, we performed a biochemical co-purification and mass spectrometry with His-tagged PGRN and His-tagged ND7 in Hsp70 deficient cells, which led to the identification of ERp57, also referred to as protein disulfide isomerase A3 (PDIA3), as a protein that binds to both PGRN and ND7. Within type 2 neuropathic GD patient fibroblasts L444P, bearing *GBA1* L444P mutation, deletion of ERp57 largely abolished the therapeutic effects of PGRN and ND7, as manifested by loss of effects on lysosomal storage, GCase activity, and β-GlcCer accumulation. Additionally, recombinant ERp57 effectively restored the therapeutic effects of PGRN and ND7 in ERp57 knockout L444P fibroblasts. Collectively, this study reports ERp57 as a previously unrecognized binding partner of PGRN that contributes to PGRN regulation of GD.

Keywords progranulin, ERp57, granulin E, GCase, Gaucher disease

1. Introduction

Gaucher disease (GD), one of the most common lysosomal storage diseases (LSDs), is caused by mutations in *GBA1* encoding GCase, which is responsible for the degradation of its substrate glucosylceramide (GCase) (*1,2*). The accumulated substrates in lysosomes lead to dysfunction of lysosomes in indicative organs (*3,4*). GD is divided into three types based on its clinical presentations (*5,6*). Type 1 non-neuropathic GD accounts for over 90% of GD patients and mainly involves macrophages of peripheral systems; patients have symptoms of anemia, bleeding, osteoporosis, and bone pain, as well as hepatosplenomegaly. Type 2 and 3, which are rare neuropathic types accounting for less than 10% of patients, affect the central nervous system as well as peripheral symptoms. Type 2 is rapidly progressive, and patients usually die before 3 years-old, while type 3 patients live to adulthood with slowly progressive neurological involvement (*7,8*). Currently, enzyme replacement therapy (ERT) is available as effective treatment for non-neuropathic GD. ERT offsets low levels of GCase enzyme with a modified version of the enzyme. However, ERT is very expensive (around $350,000/year/patient) and not effective for all patients (*9,10*). In addition, substrate reduction therapy (SRT) drugs have similarly shown clinical improvement in visceral disease parameters but have no therapeutic utility for treating neuropathic GD, because they cannot penetrate the blood-brain barrier (BBB) and are ineffective for treating neuropathic GD (nGD) (*11,12*).

Clinical symptoms may have many variations among patients carrying the same *GBA1* mutations, ranging from a life-threatening manifestation to nearly asymptomatic manifestations (*13,14*), suggesting the presence of GCase co-factor(s) whose deficiency/mutations may contribute the diverse clinical manifestations of GD. Indeed, we previously reported that ovalbumin (OVA)-challenged progranulin (PGRN) deficient mice developed GD-like phenotypes, including Gaucher cells and tubular-like

lysosomes (*15*). PGRN is a multi-faceted glycoprotein with a unique "beads-on-a-string" structure (*16-18*). PGRN can function both extracellular as a growth factor like molecule and intracellular as a critical lysosomal protein (*19-25*). Growing evidence revealed the association of PGRN with several lysosomal storage diseases, such as GD and Tay-Sachs disease (*15,26,27*). We found that PGRN bound to GCase and recruited Hsp70 to GCase through its *Grn* E domain (*15,28*). In addition, PGRN deficiency impairs the autophagy in GD (*29*). Furthermore, PGRN and its derived ND7, the C-terminal 98 amino acid fragment of PGRN bearing *Grn* E domain, could ameliorate the GD phenotypes in OVA-challenged PGRN deficient mice and GD patient fibroblasts (*28*). In addition, ND7 could cross BBB and effectively ameliorated the nGD manifestations in GD mouse models (*30*).

In the current study, we found that PGRN and ND7 still exhibit therapeutic effects against GD in Hsp70 knockout (KO) cells. We then sought to investigate the underlying mechanisms of PGRN regulation of GD in Hsp70-independent manner. Through mass spectrum (MS) and co-immunoprecipitation screening, we identified ERp57, also called protein disulfide isomerase A3 (PDIA3), is a novel binding component for both PGRN and ND7. Additionally, ERp57 deficiency abolished the therapeutic effects of PGRN and ND7, and recombinant ERp57 rescued PGRN and ND7's effects in ERp57 deficient type 2 GD patient fibroblasts.

2. Materials and Methods

2.1. Cells and Antibodies

Fibroblasts of WT and type 2 GD patients were obtained from Cornell Cel Repositories (Camden, NJ, USA). Antibodies targeted for GFP (sc-9996), His-tag (sc-57598), and GAPDH (sc-25778) were all purchased from Santa Cruz Biotechnology (Dallas, TX USA). PCDGF antibody (40–3400) was procured from Invitrogen (Waltham, MA, USA). ERp57 antibody (G117) was procured from Cell Signaling Technology (Danvers, MA, USA). All fluorescence-labeled secondary antibodies used in these experiments were purchased from Jackson Immuno Research Laboratories (West Grove, PA, USA). The substrate 4-Methylumbelliferyl β-D-glucopyranoside (4-MUG, M3633) was acquired from Sigma-Aldrich (Natick, MA, USA). The dye, LysoTracker Red DND99 (L7528), and both resins, Pierce High-Capacity Endotoxin Removal Resin (2,162,373.3) and HisPur™ Ni–NTA Resin (88,221), were all purchased from Thermo Fisher Scientific (Bridgewater, NJ, USA). The fluorescent stain, DAPI (H-1200), was acquired from VECTOR Laborato-ries (Burlingame, CA, USA). As delineated previously, the purified recombinant His-tag-PGRN protein was collected from HEK293T stable cell lines (*30*). Fetal bovine serum (FBS, 16,000-044) as well as the Dulbecco's modified Eagle's medium (DMEM; 11,965–118) were both acquired from Gibco-BRL (Waltham, MA, USA).

2.2. Cell culture

Type 2 patient fibroblasts (GM08760) with the *GBA1* genotype, L444P/L444P, were acquired from Cornell Cell Repositories (Camden, NJ, USA). HEK293T cells and L444P fibroblasts were both cultured within DMEM that is supplemented with 1% penicillin-streptomycin and 10% FBS.

2.3. Generation of ERp57 knockout cell lines using Clustered Regularly Interspaced Short PalindromicRepeats Cas-9 (CRISPR-Cas9)

The CRISPR-Cas9 genome editing technology was implemented for the deletion of ERp57 gene. The sgRNA (5′CCGACGTGCTAGAACTCACG3′) targeting the human PDIA3 genomic sequence was sub-cloned into a lentiCRISPR lentiviral plasmid following the provided protocol (Addgene, 49,535; Dr. Feng Zhang's CRISPR Depositing Lab). Preparation of the lentivirus involved cloning human ERp57 small guided (sg) RNA into lentiCRISPR plasmids followed by their transfection into HEK293 cells, which were co-transfected with both psPAX3 and pMD2.G lentiviral packaging plasmids. Following its assembly in HEK293T cells, the lentivirus produced was used to infect GD fibroblasts L444P, and individual clones were generated with drug selection (Puromycin 0.5 μg/mL) for 5–7 days. To analyze the ERp57 knockout deficiency within these selected cells, western blotting was utilized.

2.4. Western blotting

SDS-PAGE was used to separate protein samples. After gel electrophoresis, these samples were then transferred onto a nitrocellulose membrane. Upon completion of the transfer, the membrane was blocked with 5% nonfat milk for 1 h to prevent non-specific binding. After the hour, primary antibody was used to probe the membrane overnight at 4°C. The next day, Tris Buffered Saline, with Tween® 20, pH 8.0 (TBST) was used to wash the membrane before incubating the membrane with the secondary antibody. Incubation was for 1 h at room temperature with intermittent washing by TBST. In order to develop the bands on the membrane, ECL Prime Western Blotting Detection Reagent was used for visualization (Amersham, Pittsburge, PA, USA).

2.5. Preparation of lipid extraction

Mouse brain tissues were obtained and served as a source of a lipid mixture. Under sterile conditions, one mouse brain was briefly dissected. Next, 50 mL of Phosphate-

Buffered Saline (PBS) was used to homogenize the collected brain tissues. Finally, the protein level within in the brain lysates were determined using a bicinchoninic acid assay.

2.6. LysoTracker assay

WT or type 2 GD L444P patient fibroblasts were cultured on Black-clear bottom 96-well microplate and challenged with lipid lysis (50 μg/mL) plus PBS, ND7, or PGRN for 24 h. The next day, fresh medium containing 300 nM LysoTracker® Red was added for 1 h. The cells were washed with PBS. The fluorescence intensity was read by the plate reader at excitation/emission of 647/668 nm, or the live images were taken by fluorescence microscopy.

2.7. GCase activity assay

GCase enzyme activity in indicated cell lysate was determined fluorometrically with 4-methylumberlliferyl-β-D-glucopyranoside (4MU-Glc) in the presence of the GCase irreversible inhibitor, Conduritol B epoxide (CBE, 2 mM, Millipore, Bedford, MD) as previously described (*31*). Briefly, cell pellets were lysed with lysis buffer and protein concentrations of cell lysate were determined by BCA assay using BSA for normalization. GCase activity was determined by 4MU-Glc as substrate in 0.25%Tc/Tx diluted in 0.1 M citrate phosphate (CP) buffer (pH 5.6). The GCase-specific activity was calculated by subtracting background activity (with CBE) from total activity (without CBE) and normalized to total protein.

2.8. Preparation of recombinant PGRN

Generation of our recombinant PGRN stable cell line and purification of recombinant PGRN has been described in our previous publication (*24*). In brief, stable cells were cultured in DMEM that contained 1 mg/mL G418. PGRN was affinity-purified from the medium of starved cells by using nickel nitrilotriacetic-agarose. The purity of recombinant PGRN was determined by SDS-PAGE.

2.9. Expression and purification of ND7

The sequence encoding ND7, the *Grn* E, was inserted into the pD444 expression vector with a 6xHis-tag (DNA2.0, Menlo Park, CA) as described (*28*). ND7 was expressed in the BL21(DE3) *Escherichia coli* strain. Three hours after induction by 1 mM IPTG, *E. coli* cells were pelleted and sonicated to release the fusion protein. 6xHis-tagged ND7 was purified using His-Select Nickel Affinity Gel (Sigma-Aldrich, Natick, MA, USA). Briefly, *E. coli* cell lysate was incubated with affinity beads overnight and washed with washing buffer (50 mM NaH_2PO4, 200 mM NaCl, 50 mM imidazole, pH 8.0) five times. ND7 was eluted from beads with elution buffer (50 mM NaH_2PO4, 200 mM NaCl, 250 mM imidazole, pH 8.0). After dialysis with PBS, endotoxin removal using Pierce High-Capacity Endotoxin Removal Resin (Cat. No. 2162373.3) (Thermo Fisher Scientific, Bridgewater, NJ, USA), and 0.2-μm filter sterilization, recombinant ND7 protein was ready to use.

2.10. Construction of expression plasmids

cDNAs encoding either full-length human PGRN or its C-terminal *Grn* E domain were cloned into pEGFP-N1 vectors by using *EcoRI* and *BamHI* restriction sites. The construct were confrmed by DNA sequence.

2.11. Solid phase binding

First, 1 μg/mL ERp57 or BSA was coated to the plate. Then biotin-labeled BSA, PGRN, or ND7 with differing doses (0, 1, 2, 5 μg/mL) were added as bait, or recombinant ERp57 with different dose (0.2, 0.5, 1, 2, 4 μg/mL) were used as bait and 1 μg/mL recombinant PGRN or BSA was used as coating protein. These steps were followed by the addition of HRP-labeled Streptavidin and its substrates. After washing to remove the unbound streptavidin-HRP, 100 μL TMB was added to each well for 30 min in the dark followed by adding 100 μL stop solution to each well. The plate was read using an automatic plate reader at 450 nm.

2.12. Immunoprecipitation

Plasmids of GFP-tagged PGRN, its C-terminal *Grn* E domain, or GFP-vector, were transfected in HEK293T cells over 48 h. Cells were lysed by RIPA lysis, and a total of 1 mg protein was used to conduct co-immunoprecipitation (Co-IP) in each sample. Anti-GFP antibody was used to perform immunoprecipitation, and ERp57 antibody was used to probe the protein complex.

2.13. Immunofluorescence staining and confocal microscope

Fixation of culture cells was performed using 4% paraformaldehyde for 10 min, which was followed by PBS wash. Next, 0.1% Triton X-100 was used for permeabilization, then 2% normal BSA was used to block the cells for 1 h, and finally, the cells were incubated with primary antibodies overnight at 4°C. On following day, PBS was used to wash cell coverslips, which were then incubated with the indicated fluorescence-labeled secondary antibodies at room temperature for 1 hour. Soon after washing with PBS, the cell coverslips were secured onto anti-fade medium that contained DAPI. A Leica TCS SP5 confocal system was used to capture images, and Image J application was used to analyze the quantification. Briefly, to analysis the mean fluorescence intensity of the indicative color of the

whole image, the image was gray scaled to 8 bit prior to measurement. In gray scale mode, pixels are associated with a value between 1 to 255, which represents their "lightness" and corresponds to the intensity of the fluorescent signal. Next after setting desired parameters, including Area, Integrated density and Mean Grey Value et. al., the measurement can be performed. By default, measurements are made over the en-tire area of the currently-selected 2D image slice. The grey value of the measurement can be export and analyzed.

2.14. Statistical analyses

All statistical analysis was performed using GraphPad Prism 7 Software. If the data met normal distribution and the variances were equal, one-way ANOVA was used for comparison among the multiple treatment. Post-hoc analysis was performed to determine which groups are significantly different to one another. Unpaired *t*-test was also performed where appropriate. Data are shown as mean ± SD, $*p < 0.05$, $**p < 0.01$, $***p < 0.001$.

3. Results

3.1. PGRN and ND7 effectively reduced lysosomal storages in Hsp70 knockout cells

We previously reported that PGRN recruited Hsp70 to GCase and formed a ternary complex when delivering GCase to the lysosome through its C-terminal *Grn* E domain, termed as ND7 (*28*). Both PGRN and ND7 are therapeutic against GD (*28*). Herein, we treated Hsp70 KO lung epithelium cells (Figure 1A) with lipid, or lipid plus recombinant PGRN (Figure 1B, C) or ND7 (Figure 1D). The lipid stimulation markedly enhanced the lysosomal storage in Hsp70 KO cells. To our surprise, both PGRN and ND7 protein still effectively reduced lysosomal storage to a basal level without Hsp70 (Figure 1E, F), indicating that Hsp70-independent molecular mechanisms also play an important role in PGRN/ND7's therapeutic effects against GD.

3.2. ERp57 was identified as an Hsp70-independent PGRN- and ND7-binding molecule

Exploring the molecular mechanisms of PGRN's regulation of GD in an Hsp70-independent manner promoted us to identify the novel components involved in PGRN- and ND7-mediated therapeutic effects against GD. Given that both PGRN and ND7 effectively prevented lysosomal storage in Hsp70 KO cells (Figure 1), we hypothesized that key protein partners should be able to bind to both PGRN and ND7 in Hsp70-independent manner. After adding His-tagged PGRN and ND7 (5 μg/mL) to Hsp70 KO cells for 24 hours, the cell lysates were immunoprecipitated by anti-His antibody (Figure 2A). The bound proteins were identified by mass spectrum (MS) analysis. Totally, 16 hits were identified

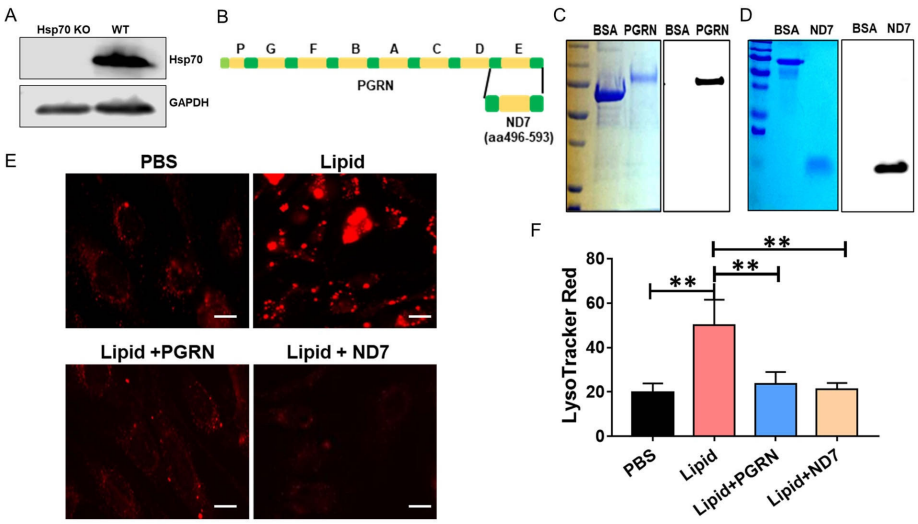

Figure 1: The effects of PGRN and ND7 on GD fibroblasts is Hsp70-independent. (A) The protein level of Hsp70 in mouse lung epithelium cells, assayed by western blotting. **(B)** Diagram of PGRN and ND7 (the 7th N-terminal deletion). PGRN regions were highlighted in yellow, which include seven and half granulin unit (P, G, F, B, A, C, D, E). The full regions linkers were highlighted in green, and half region (P) linker was highlighted in light blue, respectively. **(C)** Expression and characterization of recombinant His tagged-PGRN. His-tagged PGRN protein was purified from the HEK293 cells expressing His-PGRN using His-Select Nickel Affinity Gel. Purified PGRN was analyzed by Coomassie blue staining (left) and western blotting with PGRN antibody (right). **(D)** Expression and characterization of recombinant His tagged-ND7. Purified ND7 was analyzed by Coomassie blue staining (left) and western blotting with PGRN antibody (right). **(E)** PGRN and ND7 effectively reduce lysosomal storage in Hsp70 knockout cells. Hsp70 KO lung epithelium cells were stimulated with lipid lysis and treated with recombinant ND7 (5 μg/mL) or PGRN (10 μg/mL) for 24 h, PBS served as control. The cells were stained with LysoTracker Red. The live fluorescence microscopy imaging was taken using fluorescence microscope. **(F)** The quantification analysis of the mean florescence intensity E. Data are shown as mean ± SD of 3 independent experiments. One-way ANOVA tests. *, $p<0.05$, **, $p<0.01$. Scale bar=100 μm.

that specifically bound to both PGRN and ND7. Among the 16 hits, 7 hits were sequences related to the antibody; only 9 hits are functional proteins (Figure 2B). Among these 9 hits, identification of TCP-1 and Arpc4, two known PGRN-binding proteins (*28*), validated the technique. In addition, several RNA-binding proteins, including Sfpq, eif-4, Luc71, Alyref, Tufm, and Arglu1 were also identified as co-binding partners for PGRN and ND7 (Figure 2B). First within the protein ranking was PDIA3, which is also known as ERp57, an isomerase known to be critical for protein folding by promoting formation of disulfide bonds (*32*).

Solid phase binding assay demonstrated saturation of ERp57 binding to PGRN and ND7 (Figure 3A, B). Co-immunoprecipitation (Co-IP) further demonstrated the interaction between endogenous PGRN and ERp57 in L444P (Figure 3C). In addition, we used Nickel beads to pull down His-tagged PGRN, and then the precipitated His-tagged PGRN complex was immunoblotted onto a nitrocellulose membrane followed by detection with antibodies against ERp57. As shown in Figure 3D, ERp57 was co-purified with PGRN, further revealing the physical interaction between PGRN and ERp57.

3.3. Loss of ERp57 abolished PGRN- and its derivative ND7-mediated therapeutic effects in type 2 GD fibroblasts

Given that ERp57 is critical for promoting the formation of disulfide bonds in their glycoprotein substrates, both PGRN and ND7 are very rich in cysteine, and that ERp57 binds to both PGRN and ND7, these facts led us to hypothesize that ERp57 is important for PGRN and ND7's activities through regulating their cysteine disulfide bonds and conformation. To test this hypothesis, we deleted the ERp57 gene in type 2 GD fibroblast line *GBA1*^{L444P} (L444P) using CRISPR/Cas9 technology (Figure 4A), a powerful genome-editing approach (*33,34*). The knockout efficiency of ERp57 was confirmed using Western blot with anti-ERp57 antibody (Figure 4B). PGRN and ND7 displayed significant therapeutic effects in type 2 GD fibroblasts L444P, including reduced lysosomal storage (Figure 4C, D) and reduced accumulation of GCase substrate β-GlcCer (Figure 4E, F). However, the deletion of ERp57 abolished PGRN and ND7-mediated reduction in lysosomal storage and rescue of GCase activity in GD patient fibroblasts compared to the significant reduction of lysosomal storage and increased GCase activity after PGRN or ND7 treatment in control L444P fibroblasts (Figure 4G and H). These data indicated that loss of ERp57 abolished, at least largely, PGRN- and its derivative ND7-mediated therapeutic effect in GD fibroblasts.

3.4. Recombinant ERp57 restored the therapeutic effect of PGRN and ND7 in ERp57 deficient type 2 GD fibroblasts

Since ERp57 was identified as a binding partner of PGRN and ND7, and ERp57 deficiency ablated the therapeutic effects of PGRN and ND7 in type 2 GD patient fibroblasts L444P, including abolished their effects on lysosomal storage and GCase activity, we next examined whether addition of ERp57 in ERp57

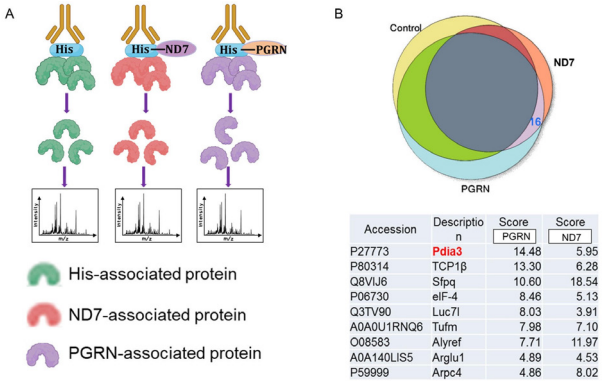

Accession	Descriptio n	Score PGRN	Score ND7
P27773	Pdia3	14.48	5.95
P80314	TCP1β	13.30	6.28
Q8VIJ6	Sfpq	10.60	18.54
P06730	eIF-4	8.46	5.13
Q3TV90	Luc7l	8.03	3.91
A0A0U1RNQ6	Tufm	7.98	7.10
O08583	Alyref	7.71	11.97
A0A140LIS5	Arglu1	4.89	4.53
P59999	Arpc4	4.86	8.02

Figure 2: ERp57 was identified as an Hsp70-independent PGRN- and ND7-binding molecule. (A) The scheme of the method used to identify potential molecules involved in PGRN- and ND7-mediated regulation of GD in Hsp70-independent manner. Immunoprecipitation was performed with His antibody from His-tagged PGRN and His-tagged ND7 treated Hsp70 KO mouse lung epithelium cells, followed by mass spectrometry. PBS treatment was used as a control. **(B)** Summary of the mass spectrometry hits that specifically bound to both PGRN and ND7.

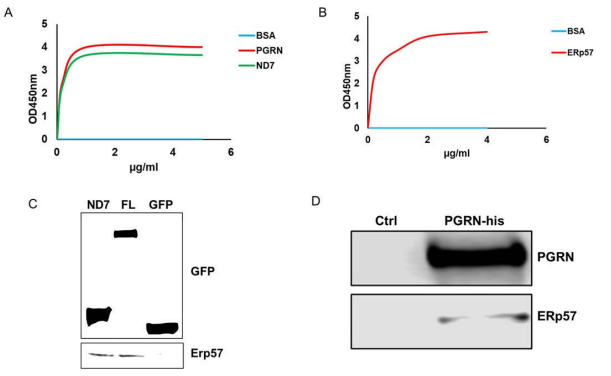

Figure 3. The identification of interaction between ERp57 and PGRN/ND7. (A) The interactions between ERp57 and PGRN/ND7, assayed by solid phase binding. Briefly, 1 μg/mL ERp57 or BSA was coated to the plate. Then biotin-labeled BSA, PGRN, or ND7 with differing doses (0, 1, 2, 5 μg/mL) were added as bait. **(B)** The interactions between ERp57 and PGRN by solid phase binding using recombinant ERp57 with different dose (0.2, 0.5, 1, 2, 4 μg/mL) as bait, and 1 μg/mL recombinant PGRN or BSA was used as coating protein. **(C)** Co-IP assay was used to examine the binding between PGRN and ERp57 in vivo. HEK293 cells were transfected with plasmids encoding GFP-fused full-length PGRN or ND7. The cell lysates were immunoprecipitated with GFP antibody. The complex was probed with ERp57 antibody. GFP-fused vector was used as a control. **(D)** Examination of the binding between PGRN and ERp57. Proteins co-purified with His-tagged PGRN were probed with ERp57 antibody. HEK293 cells transfected with His-tag vector was used as control.

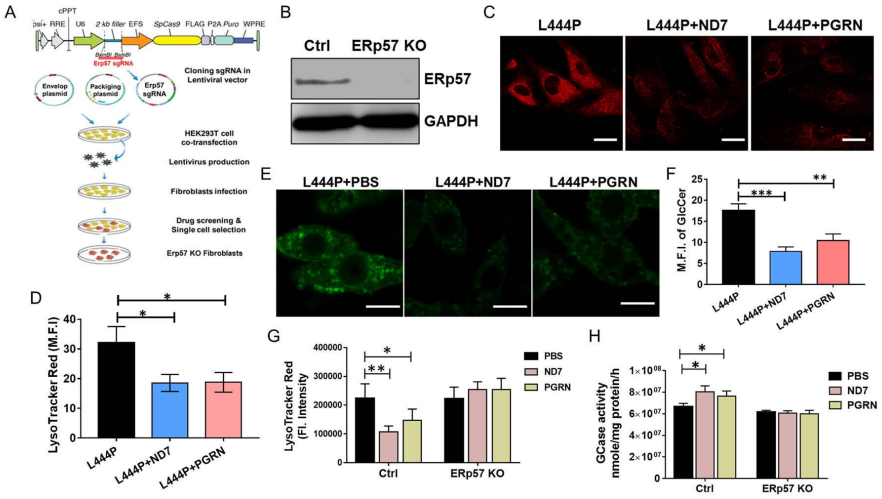

Figure 4. Deletion of ERp57 blunted the therapeutic effects of ND7 and PGRN in GD patient fibroblasts. (A) Diagram of the CRISPR/Cas9 technique for construction of human ERp57 KO GD type 2 fibroblasts L444P. **(B)** The levels of ERp57 in ERp57 KO L444P and control L444P fibroblasts, as-sayed by Western Blotting. **(C)** The lysosomal content in L444P with or without ND7 and PGRN treatment. L444P fibroblasts were stimulated with lipid lysis and treated with recombinant ND7 (5 μg/mL) or PGRN (10 μg/mL) for 24 hours. PBS used as control. The cells were stained with LysoTracker Red. The fluorescence intensity of the LysoTracker Red was determined by the live fluorescence microscopy imaging. **(D)** Quantification of mean fluorescence intensity of C analyzed using Image J. **(E)** The accumulation of β-glucosylceramide (β-GlcCer, green) in L444P fibroblasts with or without PGRN or ND7 treatment was analyzed by immunofluorescence staining with antibody against β-GlcCer. **(F)** Quantification of mean fluorescence intensity of E. **(G)** The lysosomal content in control or ERp57 KO L444P with or without ND7 and PGRN treatment. L444P fibroblasts were stimulated with lipid lysis and treated with recombinant ND7 (5 μg/mL) or PGRN (10 μg/mL) for 24 hours. PBS used as control. The cells were stained with LysoTracker Red. The fluorescence intensity of the LysoTracker Red was determined using SpectraMax i3x plate reader at excitation/emission of 647/668 nm. **(H)** The GCase activity in control or ERp57 KO L444P fibroblasts with or without ND7 and PGRN treatment were assayed by released 4MU-Glc. Data are shown as mean ± SD of 3 independent experiments. One-way ANOVA tests. *, $p<0.05$, **, $p<0.01$, ***$p<0.001$. Scale bar=100 μm.

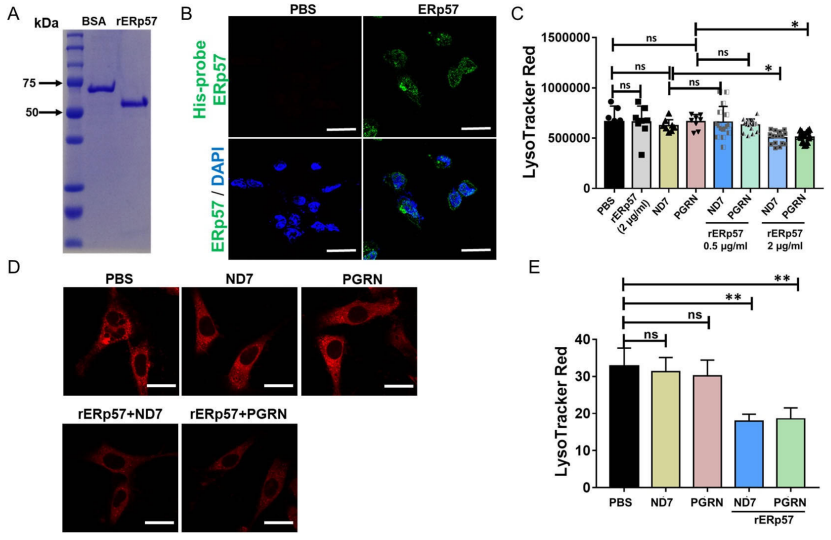

Figure 5. Recombinant ERp57 restored the effects of PGRN and ND7 on lysosomal storage in ERp57 KO L444P fibroblasts. (A) The characterization of recombinant ERp57 (rERp57) by Coomassie blue staining. **(B)** The endocytosis of rERp57. L444P fibroblasts were treated with His-tagged rERp57 (2 μg/mL) for 8 hours. The endocytosis of rERp57 was analyzed by immunofluorescence staining with antibody against His-probe. PBS was used as control. DAPI was used to stain the nuclei. **(C)** The lysosomal storage in ERp57 KO L444P. ERp57 KO L444P fibroblasts were treated with ND7 (5 μg/mL), or PGRN (10 μg/mL), or ND7/PGRN plus rERp57 (0.5 μg/mL or 2 μg/mL) for 24 hours. PBS and ERp57 (2 μg/mL) were used as controls. The fluorescence intensity of the LysoTracker Red was read using SpectraMax i3x plate reader at excitation/emission of 647/668 nm. **(D)** The live fluorescence imaging of lysosomal storage in ERp57 KO L444P fibroblasts with or without PGRN (10 μg/mL), ND7 (5 μg/mL), PGRN plus rERp57 (2 μg/mL), or ND7 plus rERp57 (2 μg/mL), measured by LysoTracker Red. PBS used as control. **(E)** Quantification of mean fluorescence intensity of D. Data are shown as mean ± SD of 3 independent experiments. One-way ANOVA tests. *, $p<0.05$, **, $p<0.01$. ns: not significant. Scale bar=100 μm.

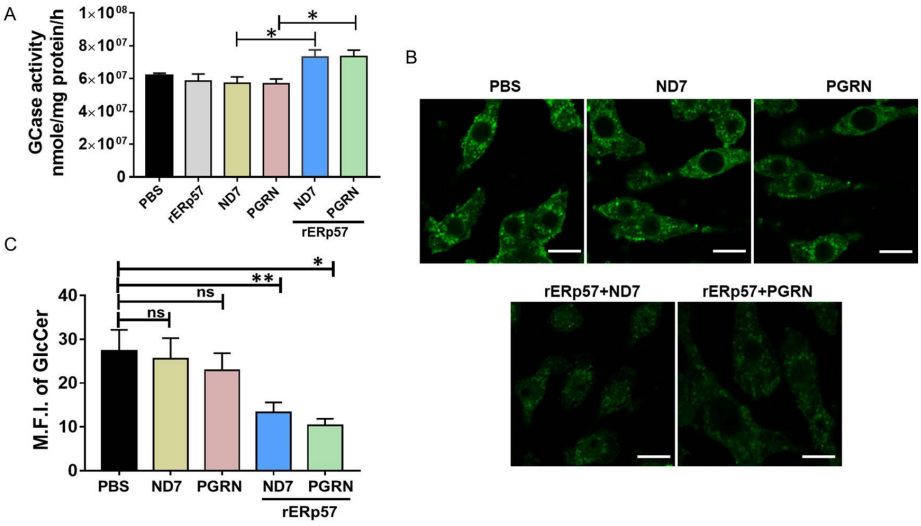

Figure 6. Recombinant ERp57 restored PGRN- and ND7-mediated increase of GCase activity and decrease of β-GlcCer accumulation in ERp57 KO L444P fibroblasts. (A) The GCase activity in ERp57 KO L444P with or without ND7 (5 μg/mL) and PGRN (10 μg/mL), or ND7 and PGRN plus rERp57 (2 μg/mL) for 24 hours. PBS and rErp57 (2 μg/mL) were used as controls. The cell lysate was used to measure the GCase activity, assayed by released 4MU-Glc. **(B)** β-GlcCer accumulation in ERp57 KO L444P with or without ND7 (5 μg/mL) and PGRN (10 μg/mL), or ND7 and PGRN plus rERp57 (2 μg/mL) for 24 hours, analyzed by immunofluorescence staining with antibody against β-GlcCer. **(C)** Quantification of mean fluorescence intensity of B. Data are shown as mean ± SD of 3 independent experiments. One-way ANOVA tests. *, $p<0.05$, **, $p<0.01$. ns: not significant. Scale bar=100 μm.

KO L444P fibroblasts could restore PGRN/ND7's therapeutic effects. For this purpose, recombinant ERp57 (rERp57) (Figure 5A) was used to treated ERp57 KO L444P fibroblasts. To teste if rERp57 could be taken up by the cells, ERp57 KO L444P fibroblasts were treated with His-tagged rERp57 (2 μg/mL) for 8 hours and then immunofluorescence staining was performed with His-probe to determine the endocytosis of ERp57. PBS was used as a control. Figure 5B clearly showed that rERp57 could be taken up by the cells, indicated by the green signals. In order to determine the optimum working dose of rERp57, ERp57 KO L444P fibroblasts were treated with PGRN and ND7, or PGRN- and ND7- plus rERp57 at different doses, 0.5 μg/mL and 2 μg/mL, respectively. We found that PGRN- or ND7- plus high dose of ERp57 (2 μg/mL) significantly decreased the lysosomal storage in ERp57 KO L444P fibroblasts, while PGRN or ND7 plus the low dose of ERp57 did not show significant changes compared with PGRN or ND7 treatment groups (Figure 5C). The high dose of ERp57 (2 μg/mL) is thus selected as the effective working dose for the further experiments.

Consequently, 2 μg/mL ERp57 was used to evaluate its mediation on the therapeutic effects of PGRN and ND7 in GD fibroblasts. In Figure 5D and E, PGRN and ND7 treatment could not rescue the lysosomal storage in ERp57 KO L444P fibroblasts, however, in the presence of ERp57 (2 μg/mL), both PGRN and ND7 significantly decreased the lysosomal content indicated by the fluoresce intensity of LysoTracker Red (Figure 5D and E). Furthermore, the GCase activity of ERp57 KO L444P fibroblasts after the treatment with PGRN or ND7 in the presence or absence of ERp57 was determined. GCase activity was not restored with PGRN or ND7 treatment in ERp57 KO L444P fibroblasts in comparison with that of the PBS control group, while it was increased significantly with PGRN or ND7 treatment in the presence of ERp57 (2 μg/mL), measured by the mean fluorescence intensity (MFI) of released 4-methylumbelliferone (Figure 6A). Accordingly, in the presence of ERp57 (2 μg/mL), PGRN or ND7 treatment reduced the β-GlcCer accumulation by approximately 50% (Figure 6B and C). Collectively, these data suggested that ERp57 is crucial for PGRN/ND7's therapeutic effects in GD fibroblast.

4. Discussion

We previously reported that PGRN is a novel modifier of GCase in GD (*15*). OVA-challenged PGRN deficiency mice developed typical GD phenotypes (*28*). Serum levels of PGRN was significantly lower in GD patients than in healthy controls (*15*). Further study showed that PGRN directly bound to GCase through its *Grn* E domain, acting as a co-chaperone of Hsp70, recruited Hsp70 to GCase and forms a ternary complex in the delivery of GCase to lysosome (*28*). Moreover, recombinant PGRN and its derived biologic ND7, which includes the full region of the *Grn* E domain, could ameliorate the GD phenotypes in OVA-challenged PGRN deficient mice and GD patient fibroblasts (*28*). Although PGRN bound to GCase through its *Grn* E

domain (ND7) and formed a complex with Hsp70, we unexpectedly found that PGRN and ND7 still displayed significant protective effects against GD in Hsp70 deficient cells. The molecular mechanisms underlying Hsp70-independent promoted us to identify the new binding partners that may mediate PGRN's and ND7's therapeutic effects against GD. Through MS and co-immunoprecipitation analysis *et al*., ERp57, an enzyme known to be important in promoting the formation of disulfide bonds and the protein folding, was identified as a novel binding partner of both PGRN and its derivative ND7 (Figure 2 and 3).

ERp57, also known as PDIA3, is a pleiotropic member of the protein disulfide isomerase (PDI) family that has attracted significant attention from researchers (*35*). ERp57 is dominantly located in the endoplasmic reticulum (ER) (*36*) as well as other cellular compartments, such as the nucleus and the cell membrane (*37,38*). ERp57 is associated with various of diseases, such as neurological disease (*39*), cancer (*40*), and infectious disease (*41*). To determine whether ERp57 could mediate PGRN/ND7's therapeutic effect in GD, we measured the GD phenotypes after PGRN and ND7 treatment in type 2 GD patient fibroblasts L444P with or without ERp57. We found that both recombinant PGRN and ND7 could ameliorate GD phenotypes in L444P fibroblast (Figure 4), consistent with the previous report (*28*). However, these therapeutic effects of PGRN and ND7 were compromised in ERp57 KO L444P fibroblasts compared with those of control L444P fibroblast (Figure 4G, H). ERp57 is an isomerase enzyme, involved in protein folding, catalyzing the formation, and critical for remodeling of disulfide bonds in their glycoprotein substrates (*42,43*). Both PGRN and ND7 are rich in cysteine; ERp57 might play a critical role in PGRN and ND7's activities by regulating their cysteine disulfide bonds and functional conformation in GD.

To prove our hypothesis, we analyzed the GD phenotypes after PGRN/ND7 treatment in the presence or absence of recombinant ERp57 in ERp57 KO L444P fibroblast. From Figure 5B, it clearly showed that rERp57 could be taken up by the cells, accordingly, the GD phenotypes in ERp57 KO fibroblasts were rescued after PGRN or ND7 plus rERp57 in comparison with no ERp57 (Figure 5 and Figure 6). These data supported our hypothesis that ERp57 play a critical role in mediating PGRN and ND7's therapeutic effects against GD.

Currently, ERT is mainly available as an effective treatment for non-neuropathic type 1 GD in clinics. However, ERT is very expensive and not effective for all patients, and especially ineffective for treating neuropathic type 2 and 3 GD patients. Approved SRT drugs have shown similar clinical improvement in visceral disease parameters but have no therapeutic utility for neuropathic GD (*9-12*). Developing an alternative treatment for GD, specifically for nGD is an urgent and unmet medical need. PGRN was identified as a novel modifier of GCase and involved in various lysosomal storage disease by previous studies, especially our recent published paper showed that PGRN derivative ND7 could penetrate BBB and protect GD and nGD pathologies in *Grn* and *Gba1* double mutant mice, another new GD mouse mode showing more severer GD phenotypes compared with the traditional GD model (*27,28,30*). Furthermore, PGRN and ND7 also ameliorated the GD phenotypes in both type 1 and type 2 GD patient fibroblasts (*31*). The previous study indicated the promising therapeutic potentials of PGRN derivative ND7 against GD. Compared with the ERT and SRT treatment for GD, ND7 showed unique functions, including BBB penetration, ameliorated GD and nGD phenotypes, and prevention of the neurodegenerative markers (*30*). In addition, the development of peptide-based drug has more advantages, including high potency, low cost and potential low toxicity, *et al*.(*44,45*). Our study showed that ERp57 plays an important role in the regulation of both PGRN and its derivative ND7, in type 2 neuropathic GD patient fibroblasts. Given that ND7 showed therapeutic effect in different GD animal models, and type 1 and type 2 GD patient fibroblast, ERp57, the identification and manipulation of this novel PGRN/ND7 binding partner may lead to innovative therapeutic for GD and other lysosomal storage diseases.

However, a few limitations to the current study were also noted. First, ERp57 mediate-therapeutic effect of PGRN or ND7 was studied only in type 2 GD patient fibroblasts, whether this meditation effect is universal need further study in other types of GD. Second, multiple does of recombinant ERp57 should be tested to find out the best working efficiency of ERp57 to rescue the therapeutic effect of PGRN and ND7 in GD. Eventually, how ERp57 exert its role once endocytosed to the cells is unclear in the study. Several hypotheses can be considered, ERp57 might escape from the endosomes and interact with PGRN to play the role, or ERp57 released to lysosome once endosome fused with lysosome and interact with PGRN in lysosomes. Having pointed out these issues, the subsequent studies, such as determine the ERp57 meditation effect of PGRN/ND7 in type 1 and type 3 GD patient fibroblast. In addition, the localization of ERp57 after endocytosed where it might exert its role is also need investigation.

In conclusion, this study reports ERp57 as a novel binding component for PGRN. ERp57 deficiency abolished the therapeutic effects of PGRN and its derivative ND7. However, the addition of recombinant ERp57 reinstated the effects of PGRN and ND7 in type 2 GD patient fibroblasts deficient in ERp57. With the consideration that ERp57 is involved in a plethora of disease processes, the identification and manipulation of this novel PGRN/ND7 binding partner may lead to innovative therapeutic for GD and other lysosomal storage diseases.

Acknowledgements

The authors would like to acknowledge all lab members for insightful discussions and critical reading. We thank Dr. Yan Deng at NYU Medical School OCS Microscopy Core for their assistance with confocal and electron microscope imaging.

Funding: This work is supported partly by NIH research grants R01NS103931, R01AR062207, R01AR061484, R01AR076900, R01AR078035, and R21OD033660.

Conflict of Interest: The authors have no conflicts of interest to disclose.

References

1. Stone DL, Tayebi N, Orvisky E, Stubblefield B, Madike V, Sidransky E. Glucocerebrosidase gene mutations in patients with type 2 Gaucher disease. Hum Mutat. 2000; 15:181-188.
2. Ankleshwaria C, Mistri M, Bavdekar A, Muranjan M, Dave U, Tamhankar P, Khanna V, Jasinge E, Nampoothiri S, Edayankara Kadangot S, Sheth F, Gupta S, Sheth J. Novel mutations in the glucocerebrosidase gene of Indian patients with Gaucher disease. J Hum Genet. 2015; 60:285.
3. Platt FM. Sphingolipid lysosomal storage disorders. Nature. 2014; 510:68-75.
4. Chen Y, Sud N, Hettinghouse A, Liu CJ. Molecular regulations and therapeutic targets of Gaucher disease. Cytokine Growth Factor Rev. 2018; 41:65-74.
5. Mistry PK, Lopez G, Schiffmann R, Barton NW, Weinreb NJ, Sidransky E. Gaucher disease: Progress and ongoing challenges. Mol Genet Metab. 2017; 120:8-21.
6. Nair S, Branagan AR, Liu J, Boddupalli CS, Mistry PK, Dhodapkar MV. Clonal Immunoglobulin against Lysolipids in the Origin of Myeloma. N Engl J Med. 2016; 374(6):555-561.
7. Stirnemann J, Belmatoug N, Camou F, Serratrice C, Froissart R, Caillaud C, Levade T, Astudillo L, Serratrice J, Brassier A, Rose C, Billette de Villemeur T, Berger MG. A Review of Gaucher Disease Pathophysiology, Clinical Presentation and Treatments. Int J Mol Sci. 2017; 18:441.
8. Desnick RJ, Barton NW, Furbish S, Grabowski GA, Karlsson S, Kolodny EH, Medin JA, Murray GJ, Mistry PK, Patterson MC, Schiffmann R, Weinreb NJ. Roscoe Owen Brady, MD: Remembrances of co-investigators and colleagues. Mol Genet Metab. 2017; 120:1-7.
9. Kirkegaard T, Gray J, Priestman DA, *et al*. Heat shock protein-based therapy as a potential candidate for treating the sphingolipidoses. Sci Transl Med. 2016; 8:355ra118.
10. Lukina E, Watman N, Dragosky M, Pastores GM, Arreguin EA, Rosenbaum H, Zimran A, Angell J, Ross L, Puga AC, Peterschmitt JM. Eliglustat, an investigational oral therapy for Gaucher disease type 1: Phase 2 trial results after 4 years of treatment. Blood Cells Mol Dis. 2014; 53:274-276.
11. Kuter DJ, Mehta A, Hollak CE, Giraldo P, Hughes D, Belmatoug N, Brand M, Muller A, Schaaf B, Giorgino R, Zimran A. Miglustat therapy in type 1 Gaucher disease: clinical and safety outcomes in a multicenter retrospective cohort study. Blood Cells Mol Dis. 2013; 51:116-124.
12. Bennett LL, Mohan D. Gaucher disease and its treatment options. Ann Pharmacother. 2013; 47:1182-1193.
13. Weiss K, Gonzalez A, Lopez G, Pedoeim L, Groden C, Sidransky E. The clinical management of Type 2 Gaucher disease. Mol Genet Metab. 2015; 114:110-122.
14. Staretz-Chacham O, Choi JH, Wakabayashi K, Lopez G, Sidransky E. Psychiatric and behavioral manifestations of lysosomal storage disorders. Am J Med Genet B Neuropsychiatr Genet. 2010; 153B:1253-1265..
15. Jian J, Zhao S, Tian QY, *et al*. Association Between Progranulin and Gaucher Disease. EBioMedicine. 2016; 11:127-137.
16. Hrabal R, Chen Z, James S, Bennett HP, Ni F. The hairpin stack fold, a novel protein architecture for a new family of protein growth factors. Nat Struct Biol. 1996; 3:747-752.
17. Palfree RG, Bennett HP, Bateman A. The Evolution of the Secreted Regulatory Protein Progranulin. PLoS One. 2015; 10:e0133749.
18. Tolkatchev D, Malik S, Vinogradova A, Wang P, Chen Z, Xu P, Bennett HP, Bateman A, Ni F. Structure dissection of human progranulin identifies well-folded granulin/epithelin modules with unique functional activities. Protein Sci. 2008; 17:711-724.
19. Li SS, Zhang MX, Wang Y, Wang W, Zhao CM, Sun XM, Dong GK, Li ZR, Yin WJ, Zhu B, Cai HX. Reduction of PGRN increased fibrosis during skin wound healing in mice. Histol Histopathol. 2019; 34:765-774.
20. Jian J, Konopka J, Liu C. Insights into the role of progranulin in immunity, infection, and inflammation. J Leukoc Biol. 2013; 93:199-208.
21. Bateman A, Bennett HP. The granulin gene family: from cancer to dementia. Bioessays. 2009; 31:1245-1254
22. Kao AW, McKay A, Singh PP, Brunet A, Huang EJ. Progranulin, lysosomal regulation and neurodegenerative disease. Nat Rev Neurosci. 2017; 18:325-333.
23. Cui Y, Hettinghouse A, Liu CJ. Progranulin: A conductor of receptors orchestra, a chaperone of lysosomal enzymes and a therapeutic target for multiple diseases. Cytokine Growth Factor Rev. 2019; 45:53-64.
24. Tang W, Lu Y, Tian QY, *et al*. The growth factor progranulin binds to TNF receptors and is therapeutic against inflammatory arthritis in mice. Science. 2011; 332:478-484.
25. Zhao X, Hasan S, Liou B, Lin Y, Sun Y, Liu C. Analysis of the Biomarkers for Neurodegenerative Diseases in Aged Progranulin Deficient Mice. Int J Mol Sci. 2022; 23:629.
26. Jian J, Hettinghouse A, Liu CJ. Progranulin acts as a shared chaperone and regulates multiple lysosomal enzymes. Genes Dis. 2017; 4:125-126.
27. Chen Y, Jian J, Hettinghouse A, Zhao X, Setchell KDR, Sun Y, Liu CJ. Progranulin associates with hexosaminidase A and ameliorates GM2 ganglioside accumulation and lysosomal storage in Tay-Sachs disease. J Mol Med (Berl). 2018; 96:1359-1373.
28. Jian J, Tian QY, Hettinghouse A, Zhao S, Liu H, Wei J, Grunig G, Zhang W, Setchell KDR, Sun Y, Overkleeft HS, Chan GL, Liu CJ. Progranulin Recruits HSP70 to β-Glucocerebrosidase and Is Therapeutic Against Gaucher Disease. EBioMedicine. 2016; 13:212-224.
29. Zhao X, Liberti R, Jian J, Fu W, Hettinghouse A, Sun Y, Liu CJ. Progranulin associates with Rab2 and is involved in autophagosome-lysosome fusion in Gaucher disease. J Mol Med (Berl). 2021; 99:1639-1654.

30. Zhao X, Lin Y, Liou B, Fu W, Jian J, Fannie V, Zhang W, Setchell KDR, Grabowski GA, Sun Y, Liu CJ. PGRN deficiency exacerbates, whereas a brain penetrant PGRN derivative protects, GBA1 mutation-associated pathologies and diseases. Proc Natl Acad Sci U S A. 2023; 120:e2210442120.
31. Liou B, Zhang W, Fannin V, Quinn B, Ran H, Xu K, Setchell KDR, Witte D, Grabowski GA, Sun Y. Combination of acid β-glucosidase mutation and Saposin C deficiency in mice reveals Gba1 mutation dependent and tissue-specific disease phenotype. Sci Rep. 2019; 9:5571.
32. Hirano N, Shibasaki F, Sakai R, Tanaka T, Nishida J, Yazaki Y, Takenawa T, Hirai H. Molecular cloning of the human glucose-regulated protein ERp57/GRP58, a thiol-dependent reductase. Identification of its secretory form and inducible expression by the oncogenic transformation. Eur J Biochem. 1995; 234:336-342.
33. Long C, McAnally JR, Shelton JM, Mireault AA, Bassel-Duby R, Olson EN. Prevention of muscular dystrophy in mice by CRISPR/Cas9-mediated editing of germline DNA. Science. 2014; 345:1184-1188.
34. Maddalo D, Manchado E, Concepcion CP, Bonetti C, Vidigal JA, Han YC, Ogrodowski P, Crippa A, Rekhtman N, de Stanchina E, Lowe SW, Ventura A. *In vivo* engineering of oncogenic chromosomal rearrangements with the CRISPR/Cas9 system. Nature. 2014; 516:423-427.
35. Hettinghouse A, Liu R, Liu CJ. Multifunctional molecule ERp57: From cancer to neurodegenerative diseases. Pharmacol Ther. 2018; 181:34-48.
36. Grillo C, D'Ambrosio C, Scaloni A, Maceroni M, Merluzzi S, Turano C, Altieri F. Cooperative activity of Ref-1/APE and ERp57 in reductive activation of transcription factors. Free Radic Biol Med. 2006; 41:1113-23.
37. Grindel BJ, Rohe B, Safford SE, Bennett JJ, Farach-Carson MC. Tumor necrosis factor-α treatment of HepG2 cells mobilizes a cytoplasmic pool of ERp57/1,25D$_3$-MARRS to the nucleus. J Cell Biochem. 2011; 112:2606-2615.
38. Chichiarelli S, Altieri F, Paglia G, Rubini E, Minacori M, Eufemi M. ERp57/PDIA3: new insight. Cell Mol Biol Lett. 2022; 27:12.
39. Bargsted L, Hetz C, Matus S. ERp57 in neurodegeneration and regeneration. Neural Regen Res. 2016; 11:232-233.
40. Powell LE, Foster PA. Protein disulphide isomerase inhibition as a potential cancer therapeutic strategy. Cancer Med. 2021; 10:2812-2825.
41. Wu J, Wang Y, Wei Y, Xu Z, Tan X, Wu Z, Zheng J, Liu GD, Cao Y, Xue C. Disulfide isomerase ERp57 improves the stability and immunogenicity of H3N2 influenza virus hemagglutinin. Virol J. 2020; 17:55.
42. Turano C, Gaucci E, Grillo C, Chichiarelli S. ERp57/GRP58: a protein with multiple functions. Cell Mol Biol Lett. 2011; 16:539-563.
43. Bechtel TJ, Weerapana E. From structure to redox: The diverse functional roles of disulfides and implications in disease. Proteomics. 2017; 17:10.1002/pmic.201600391.
44. Craik DJ, Fairlie DP, Liras S, Price D. The future of peptide-based drugs. Chem Biol Drug Des. 2013; 81:136-147.
45. Luo X, Chen H, Song Y, Qin Z, Xu L, He N, Tan Y, Dessie W. Advancements, challenges and future perspectives on peptide-based drugs: Focus on antimicrobial peptides. Eur J Pharm Sci. 2023; 181:106363.

Received February 6, 2023; Revised March 1, 2023; Accepted March 6, 2023.

[§]These authors contributed equally to this work.
**Address correspondence to:*
Chuanju Liu, Department of Orthopaedic Surgery, NYU Grossman School of Medicine, 301 East 17th Street, New York, NY 10003, USA.
E-mail: chuanju.liu@nyulangone.org

Released online in J-STAGE as advance publication March 9, 2023.